Luminescence 2006; 21: 7–14
Published online 3 August 2005 in Wiley InterScience (www.interscience.wiley.com). DOI: 10.1002/bio.874 *ORIGINAL RESEARCH*

Fluorescence anisotropy studies of molecularly imprinted polymers

Yin-Chu Chen,[1] Zheming Wang,[2] Mingdi Yan[3] and Scott A. Prahl[1]*

[1]Department of Biomedical Engineering, Oregon Health and Science University, Portland, OR, USA
[2]Environmental Molecular Sciences Laboratory, Pacific Northwest National Laboratory, Richland, WA, USA
[3]Department of Chemistry, Portland State University, Portland, OR, USA

Received 15 November 2004; revised 5 May 2005; accepted 20 May 2005

ABSTRACT: A molecularly imprinted polymer (MIP) is a biomimetic material that can be used as a biochemical sensing element. We studied the steady-state and time-resolved fluorescence and fluorescence anisotropy of anthracene-imprinted polyurethane. We compared MIPs with imprinted analytes present, MIPs with the imprinted analytes extracted, MIPs with rebound analytes, non-imprinted control polymers (non-MIPs) and non-MIPs bound with analytes to understand MIP's binding behaviour. MIPs and non-MIPs had similar steady-state fluorescence anisotropy in the range 0.11–0.24. Anthracene rebound in MIPs and non-MIPs had a fluorescence lifetime of $\tau = 0.64$ ns and a rotational correlation time of $\phi_F = 1.2$–1.5 ns, both of which were shorter than that of MIPs with imprinted analytes present ($\tau = 2.03$ ns and $\phi_F = 2.7$ ns). The steady-state anisotropy of polymer solutions increased exponentially with polymerization time and might be used to characterize the polymerization extent *in situ*. Copyright © 2005 John Wiley & Sons, Ltd.

KEYWORDS: steady-state anisotropy; time-resolved anisotropy; time-resolved fluorescence; polymerization kinetics; anthracene sensing

INTRODUCTION

Molecularly imprinted polymers (MIPs) are biomimetic materials that are used as recognition elements in biosensors. Through host–guest interactions, imprinted polymers can exhibit recognition capabilities comparable to those of antibody–antigen systems (1). The advantages of MIPs include their stability in a wide range of environments, their facility for sensor microfabrication, and their ability to detect analytes that are difficult or impossible to sense by immunoassay (2). MIPs have been used in various separation techniques (3, 4), in drug discovery processes (5) and in biochemical sensors (6–8).

The recognition properties of MIPs arise during their synthesis. In this process, functional and cross-linking monomers are co-polymerized in the presence of the target analyte (the molecule for imprinting, whose structure serves as a pattern for recognition by shape and size) (9). A good MIP system is specific to the target analytes and binds strongly with the analytes for *in situ* sensing (2, 10) or filtering (11), as well as having a high imprinting efficiency (i.e. the ratio of useful binding sites to the total number of imprinted binding sites) and uniform binding sites (12). To examine MIP's binding performance, one often relies on the fluorescence signals of bound analytes (13) or polymers (14). Steady-state fluorescence reveals the presence of analytes but lacks detailed information about the local binding environments. Moreover, if the fluorescence spectra of the analyte and the imprinted polymers overlap, it is difficult to distinguish steady-state fluorescence signals of both species (15). However, their fluorescence lifetimes and anisotropies may be different.

The fluorescence lifetime of a fluorophore depends on the fluorophore's local environment, such as degrees of freedom, degree of rotational diffusion, or the distance between the fluorophore and the absorbing molecule (16). Few research groups have studied the time-resolved fluorescence of MIPs (14, 17). Wandelt *et al.* incorporated fluorescent monomers into cAMP-imprinted polymers and detected the quenching of fluorescence of the polymer itself as the cAMP bound with the MIPs (14). Their results showed different fluorescence lifetime distributions between specific and non-specific bindings; this suggests that time-resolved fluorescence measurements could possibly be used to characterize the binding specificity of MIPs.

Fluorescence anisotropy has been used to investigate fluorescent molecules in various polymer concentrations or viscosity environments (18–21), but has not yet been used to characterize MIPs. We studied both

*Correspondence to: S. A. Prahl, 9205 SW Barnes Rd., Portland, OR 97225, USA.
E-mail: prahl@bme.ogi.edu
Contract/grant sponsor: National Instituties of Health, USA; Contract/grant number: NIH-CI-R24-CA84587-03.

the steady-state and time-resolved fluorescence and fluorescence anisotropy of MIPs. We compared the fluorescence anisotropy of MIPs with imprinted analytes present, MIPs with the imprinted analytes extracted, MIPs with rebound analytes, non-imprinted control polymers (non-MIPs) and non-MIPs bound with analytes. We also investigated changes in the steady-state anisotropy of MIPs and non-MIPs during polymerization.

MATERIALS AND METHODS

Materials

Polyurethane imprinted with anthracene was chosen as the MIP system (13, 15). MIPs were made from a mixture of 0.026 mmol anthracene, monomers (0.375 mmol bisphenol A and 0.455 mmol *p,p′*-diisocyanatodiphenylmethane) and cross-linkers (0.250 mmol trihydroxybenzene and 0.195 mmol *p,o,p′*-triisocyanatodiphenylmethane) in a total of 2 mL dimethylformamide (DMF) solution. Non-imprinted polymers were prepared in a similar manner as the MIP, except the template molecule anthracene was omitted from the solution.

1.5×1.5 cm^2 silicon wafers were first cleaned with piranha solution (100 mL 98% H_2SO_4 with 43 mL H_2O_2). Additional silanization with an amino-silane was required to covalently attach MIPs to the wafers (22). This was accomplished by immersing the clean wafers in 47 mL 1.0 mmol/L acidic methanol solution (glacial acetic acid in methanol), 2.5 mL MilliQ H_2O and 500 µL 3-aminopropyltrimethoxysilane. The reaction vessel was covered with aluminium foil and was continually flushed with nitrogen for 15 min. The wafer was then rinsed three or four times with fresh methanol to remove excess silane and subsequently heated at 120°C for 5 min to promote a complete condensation reaction. The wafer was rinsed with methanol and dried under a stream of nitrogen.

Freshly prepared mixtures of the imprinting or non-imprinting solutions were spin-coated onto the silanized silicon wafers at 1000 r.p.m. One day after the MIPs films were formed, the imprinted anthracene was extracted by soaking the MIP wafers in toluene. The fluorescence of the extraction solution was measured (excitation 365 nm, emission 404 nm) to monitor the extraction process. The toluene was replaced each day. It took about 2 days to complete the extraction process. The non-imprinted polymer samples were not treated with this procedure.

Rebinding of anthracene was conducted by soaking the extracted MIP or non-MIP samples separately in a 10 mL 0.5 mmol/L anthracene solution in DMF, sealed with aluminium foil and shaken for 2 days. Afterwards, the samples were rinsed with DMF, and dried for 1 day.

Six different types of samples were tested (3–5 replicates/sample). Table 1 summarizes the types and the number of samples tested in our study. Note that the terminology for the sample used throughout this manuscript is the abbreviated name in the table.

Experimental details

Steady-state fluorescence anisotropy measurements. The polarized fluorescence of anthracene solutions and MIP samples was measured using a fluorimeter (Fluorolog3, SPEX) with a 387 nm low-pass filter (387 AELP, Omega Optical Inc., Brattleboro, VM, USA), two polarizers and a scrambler, as shown in Fig. 1. One quartz polarizer was placed at the window of an excitation monochromator; the other polarizer was located at the emission window, at 90° to the excitation light. The 387 nm low-pass filter was placed at the excitation window immediately before the vertical polarizer to reject any possible reflected or scattered excitation light from the sample surface that might have contributed to the emission signals (16). A polarization scrambler was inserted after the second polarizer to depolarize the light and to avoid detector bias for the two polarized states.

The G-factor of the system was 1.04 ± 0.01, which was measured with anthracene in cyclohexane frozen at 77°K. Furthermore, to ensure that the instrument performed normally each time, an anthracene solution in DMF (0.1 mmol/L) inside a cuvette was measured at room temperature as a secondary check before we started the MIP measurements. The parallel and perpendicular fluorescence, $I_{\parallel}^{\mathrm{DMF}}$ and $I_{\perp}^{\mathrm{DMF}}$, of anthracene

Table 1. Summary of samples tested

Abbreviated name	Sample number	Full description
Anthracene in DMF	1	0.1 mmol/L anthracene solution in DMF
Non-MIPs	5	Non-imprinted control polyurethane
MIPs	5	MIPs with 13 mmol/L anthracene imprinted
Extracted-MIPs	4	MIPs with imprinted anthracene extracted
Rebound-MIPs	3	Extracted-MIPs rebound with anthracene
Rebound-non-MIPs	3	Non-imprinted control polyurethane rebound with anthracene

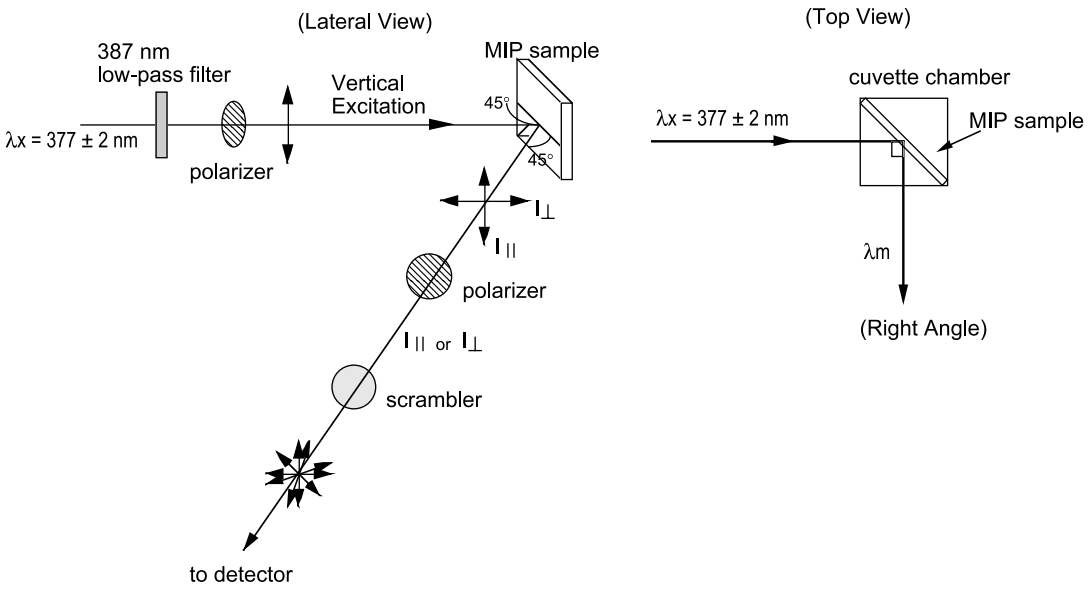

Figure 1. Schematic of the steady-state fluorescence anisotropy apparatus. Excitation light was vertically polarized and incident at an angle of 45° relative to the plane of the MIP samples. Fluorescence emission was collected at an angle of 90° relative to the incident light.

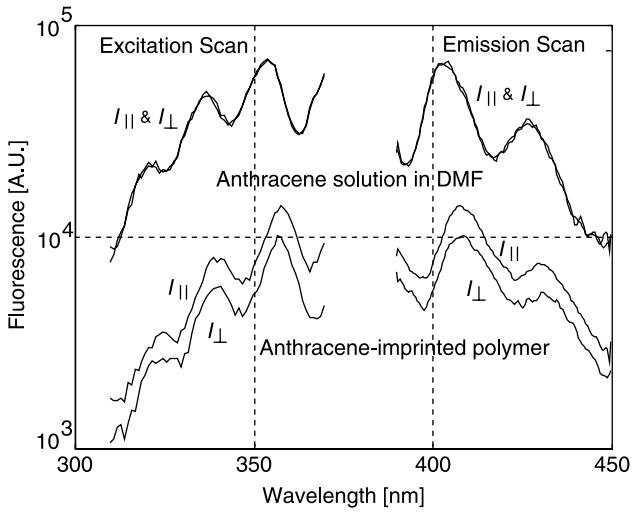

Figure 2. The perpendicular $I_{\perp}$ and parallel $I_{\parallel}$ polarized fluorescence of MIPs and anthracene in DMF for excitation scan and emission scan. The perpendicular and parallel fluorescence scans for the anthracene in DMF overlap.

in DMF should be identical, since the steady-state anisotropy of anthracene molecules in a free-rotation liquid is zero. This was found to hold for our measurements (as shown in Fig. 2 and in Results), therefore there was no bias in our instrument.

MIP samples were placed diagonally in the cuvette chamber, as shown in Fig. 1. The excitation scans used vertically polarized (relative to the plane of the table) excitation light, 310–380 nm; parallel ($I_{\parallel}$) and perpendicular ($I_{\perp}$) polarized emission at 405 ± 2.5 nm were recorded sequentially. Emission scans used 377 ± 2 nm vertically-polarized excitation light; both $I_{\parallel}$ and $I_{\perp}$ were scanned from 390 to 480 nm sequentially.

Time-resolved fluorescence anisotropy measurements. Time-resolved fluorescence measurements were conducted using a regeneratively amplified Ti:Sapphire laser system (Clark-MXR, Inc. ORC-1000 Nd:YAG pumped TRA-1000 Ti:Sapphire laser) coupled to a Hamamatsu C5680 high-speed streak-camera equipped with a M5678 Synchronous Blanking unit and 5675 Synchronous Sweep unit. The pulse duration of the laser was 110 fs. The instrument response was about 200 ps FWHM, as determined using a standard scattering alumina suspension. The set-up was similar to the steady-state measurement set-up, except that a pulsed laser and a different detector were used. An extra 420 ± 10 nm band-pass filter was placed in front of the entrance slit of the camera. A 377 ± 5 nm pulsed laser running at 76 MHz was used to excite the MIP samples and the emitted light was recorded every 0.1 ns for 50 ns. The two polarized states, $I_{\parallel}$ and $I_{\perp}$, of the emission were recorded sequentially. Two of each type of sample were measured.

Steady-state anisotropy measurements of MIP during polymerization

In this experiment, we measured the steady-state fluorescence anisotropy as a function of polymerization time of 2 mL freshly prepared MIP mixtures containing 0.011 mmol anthracene and in 2 mL non-MIPs solutions in a clear quartz cuvette, using the same set-up as in

Fig. 1. Measurements were made every 2 min for the first 10 min, every 5 min for the next 20 min, and every 1–2 hours thereafter. Samples were in a gelatinous form at this time. Five samples for each concentration of solution were measured.

DATA ANALYSIS

Time-resolved fluorescence

An exponential decay curve was used to fit the parallel-polarized fluorescence, $I_{||}(t)$, to calculate the fluorescence lifetime, τ:

$$I_{||}(t) = I_p \exp(-t/\tau) + I_0 \quad (1)$$

where I_p is the maximum fluorescence pulse irradiance and I_0 is the background light irradiance, which was calculated by averaging the fluorescence signals over the last 10 ns of recording time. Only one exponential time constant, τ, was needed because the second or higher exponential components were zero in our results.

Time-resolved fluorescence anisotropy

The fluorescence anisotropy, r, was calculated as:

$$r(t) = \frac{I_{||}(t) - I_{\perp}(t)}{I_{||}(t) + 2I_{\perp}(t)}. \quad (2)$$

For steady-state fluorescence anisotropy, $I_{||}(t)$, $I_{\perp}(t)$ and $r(t)$ are constant over time. The time-resolved anisotropy $r(t)$ was fitted to a two-component hindered-rotor model (16):

$$\frac{r(t)}{r_{\text{limit}}} = \alpha \exp\left(-\frac{t}{\phi_F}\right) + (1-\alpha)\exp\left(-\frac{t}{\phi_S}\right), \quad (3)$$

where ϕ_F is a measure of rapid rotational motions with proportion α, ϕ_S measures slower rotational motions with proportion $1-\alpha$, and r_{limit} is the limiting anisotropy. All the fittings were obtained using the fmin function of Matlab.

Anisotropy vs. polymerization time

A exponential polymerization kinetics model (23, 24) was used to relate the anisotropy $r(t)$ as a function of the polymerization time:

$$r(t) = r_{\max} - (r_{\max} - r_0)\exp\left(-\frac{t}{t_{\text{polymer}}}\right) \quad (4)$$

where $r_{\max}$ is the maximum anisotropy, r_0 is the initial anisotropy and t_{polymer} is the characteristic time for polymerization.

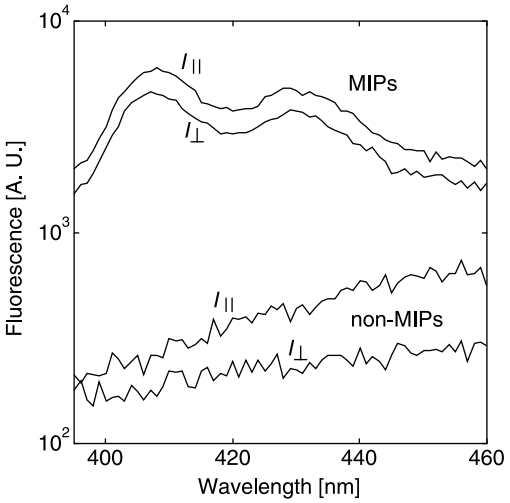

Figure 3. Comparison of the perpendicular and parallel polarized fluorescence of non-MIPs, and MIPs with 25 mmol/L anthracene imprinted. The non-MIPs emitted about 10 times less fluorescence than the MIPs.

RESULTS

Steady-state anisotropy

Fig. 2 shows the parallel and perpendicular components of excitation and emission of MIPs and the anthracene in DMF. Fluorescence of anthracene in MIPs has a 6 nm Stokes' shift relative to that in DMF. This is typical for compounds with a $S^*_{\pi\pi}$–S_0 transition in a polar solvent. Increasing the polarity of the solvent will increase the amount of red shift, but typically no more than a few nanometers (25).

Fig. 3 compares the fluorescence signals from the polymer itself (the non-MIPs samples in Table 1) and from the anthracene plus the polymers (the MIPs samples in Table 1). The non-MIPs emitted about 10 times less fluorescence than the MIPs with 25 mmol/L anthracene. The fluorescence intensity from MIPs imprinted with 1 mmol/L anthracene was at about the same level as the background signals from the polyurethane itself (non-MIPs). Therefore, anthracene at less than 1 mmol/L in MIPs was not detectable for this type of detection system.

The fluorescence anisotropy as a function of wavelength was essentially constant over the range 400–450 nm. The average anisotropy over the range 408 ± 5 nm is shown in Fig. 4. There was no significant difference in anisotropies among all the MIPs based on ANOVA at $p = 0.05$.

Time-resolved fluorescence and anisotropy

The fitted fluorescence lifetime τ in eq. 1 for the parallel-polarized fluorescence at 420 ± 10 nm of all the samples is listed in Table 2. Both rebound MIPs

Table 2. Values of the fitting parameters in Eq. 3 and their standard errors for anisotropy decays

	τ [ns]	r_{limit} [–]	α	ϕ_F [ns]	ϕ_S [ns]
Non-MIPs	3.54 ± 0.09	0.019 ± 0.001	0.995	3.4 ± 0.1	350
MIPs	2.03 ± 0.01	0.018 ± 0.001	0.95	2.7 ± 0.1	8.0 ± 0.5
Rebound-MIPs	0.63 ± 0.01	0.025 ± 0.001	0.94	1.2 ± 0.1	11.5 ± 0.5
Rebound-non-MIPs	0.64 ± 0.01	0.008 ± 0.001	0.85	1.5 ± 0.1	110 ± 5
Anthracene in DMF	4.52 ± 0.01	0 ± 0.0006			
Extracted-MIPs	9.0 ± 0.5	0 ± 0.0006			

τ, parallel-polarized fluorescence lifetime; ϕ_F and ϕ_S, fast and slow rotational correlation times, respectively; α and $1 - \alpha$, proportions of contribution; r_{limit}, limiting anisotropy.

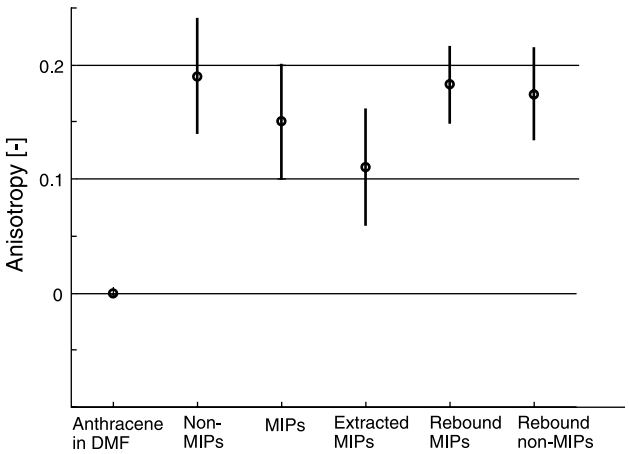

Figure 4. The steady-state fluorescence anisotropies of anthracene in DMF, non-MIPs, MIPs, extracted MIPs, rebound MIPs and rebound non-MIPs.

and rebound non-MIPs have the shortest fluorescence lifetime, while non-MIPs have the longest fluorescence lifetime (based on ANOVA at $p = 0.05$).

The fitting of eq. 3 to the anisotropies as a function of time $r(t)$ (Fig. 5) is listed in Table 2. Generally, rebound MIPs have the highest limiting anisotropy, r_{limit}, and the shortest fast-rotation correlation time, ϕ_F. The non-imprinted polyurethane has the longest fast-rotation correlation time.

Steady-state anisotropy of MIPs during polymerization

The fluorescence anisotropy of the polymers was -0.04 ± 0.04 when MIP or non-MIP solutions were freshly made. The anisotropy increased as the polymerization progressed (Fig. 6), and finally reached a stable value after the polymers solidified. Overall, the anisotropies as a function of polymerization time fitted eq. 4 with <10% standard error (Table 3).

DISCUSSION

Generally, the fluorescence anisotropy is independent of the emission wavelength because almost all emission is from the lowest singlet state (16). The steady-state anisotropy of a fluorophore in a frozen solution without rotational diffusion is given by (16):

$$r = \frac{2}{5}\left(\frac{3\cos^2\beta - 1}{2}\right)$$

where β is the angular displacement between the excitation dipole and emission dipole. Slightly lower values of r than 0.39 (corresponding to $\beta = 7.4°$) are frequently reported for dilute fluorophore solutions (16). Our anisotropy values are smaller, suggesting a larger angular displacement (an r of 0.15 corresponds to $\beta = 40°$). This is probably due to radiative reabsorption between the bound anthracene and the polyurethane matrix. The large standard deviations of the anisotropy values may be caused by the inhomogeneous distribution of the distances between these fluorophore molecules.

The steady-state anisotropy values of the MIPs and non-MIPs were not zero (Fig. 4), indicating that a MIP does not allow the anthracene to rotate freely. Therefore, the MIP acted as a solid medium where rotational diffusion was constrained for bound analytes. One concern is that the solvent (DMF) did not evaporate completely and existed as localized inclusions, which created micro- or nano-scale solvent cages in which the fluorophore was dissolved (26). It is possible that the molecular forces between such micro-/nano-scale solvent inclusion and the host environment (the MIPs) were stronger than that between the fluorophore and the bulk solvent. However, further experiments are necessary to characterize the amount of residual DMF.

The fluorescence lifetime at 420 nm emission with 377 nm excitation is 4.52 ns for 0.1 mmol/L anthracene in DMF. According to the literature (16, 27), a 1 mmol/L solution of anthracene in degassed cyclohexane had a fluorescence lifetime of 5.15 ± 0.05 ns for emission >400 nm with 365 nm excitation, and a 5 μmol/L, non-degassed solution has 3.99 ± 0.03 ns lifetime at 415 nm emission with 355 nm excitation.

The fluorescence lifetime of anthracene in a polymer system was shorter than that of anthracene in DMF. Shortening of the fluorescence lifetime is mostly caused by rapid resonance energy transfer (16) between the

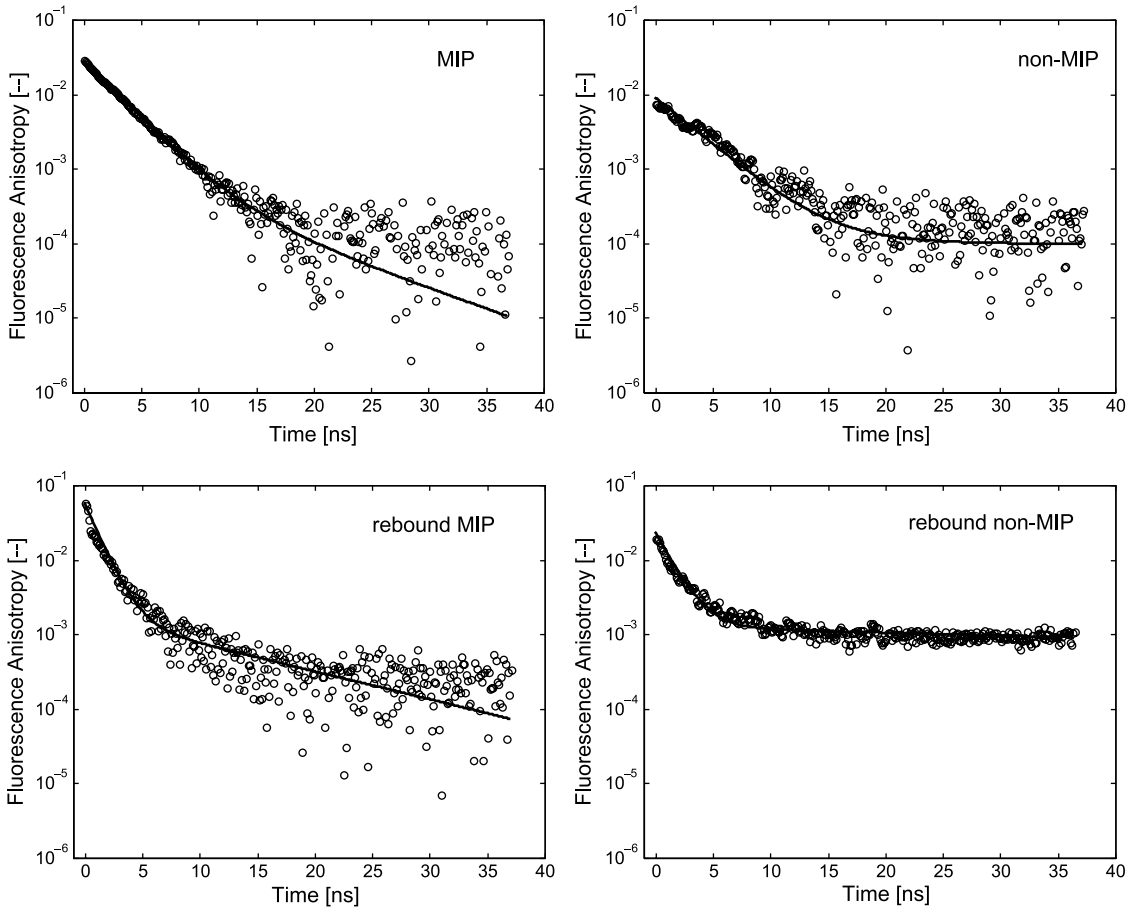

Figure 5. The fitting of the fluorescence anisotropy decay (circles) with two-exponential decay curve eq. 3 (line). Parameters of the fitted curves are presented in Table 2.

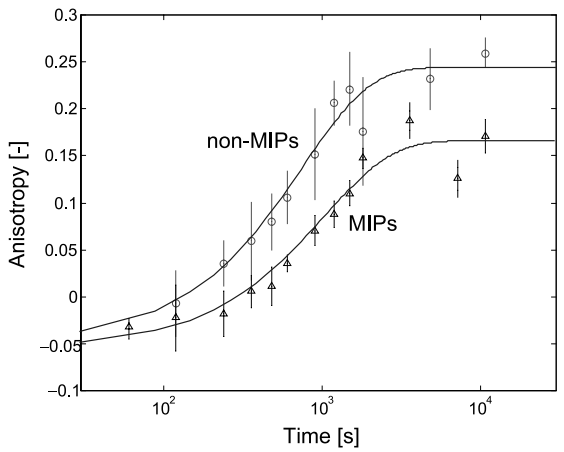

Figure 6. The fluorescence anisotropy of non-MIPs (circle) and MIPs (triangle) as a function of polymerization time. The solid curves are eq. 4 with the fitted values of Table 3.

Table 3. Values of the fitting parameters and their standard errors for MIP polymerization kinetics (eq. 4)

	r_{max}	r_0	$t_{polymer}$ (s)
Non-MIPs	0.24 ± 0.04	-0.05 ± 0.02	750 ± 150
MIPs	0.16 ± 0.05	-0.06 ± 0.03	1000 ± 400

r_{max}, maximum anisotropy; r_0, initial anisotropy; $t_{polymer}$, characteristic time for polymerization.

excited and ground-state fluorophore molecules. This is especially likely in this imprinted polyurethane medium because the polyurethane is strongly absorbent.

According to Förster theory, the efficiency of energy transfer is proportional to d^{-6}, where d is the Förster distance between the photon donor (emission dipole) and acceptor (absorbing dipole) (16). Therefore, the rate of fluorescence decay is sensitive to the binding distances between the dipoles. The fluorescence lifetime for rebound-MIPs or rebound non-MIPs was only 0.64 ns, much shorter than the 2.03 ns of the original MIP samples (Table 2). This suggests that rebound anthracene binds closely to the polymer or possibly forms localized agglomerates or aggregates on the polymer surface, causing fast energy transfer from the anthracene to the polymer or to another anthracene molecule. Further investigation is needed to quantitate the distances between the fluorophores.

Anthracene in MIP environments had fast correlation times of 1.2–2.7 ns, with limiting anisotropy ranging over 0.008–0.025 (Table 2). Pokorná *et al.* measured a

correlation time of 2.9–4.7 ns with limiting anisotropy 0.02–0.03 for anthracene in poly(methyl methacrylate) using three different solvents (chloroform, DMF and 1,4-dioxane) (20). Kudryasheva *et al.* studied the binding between the anthracene and luciferase and obtained a correlation time of 3.7–7.7 ns with limiting anisotropy of 0.13 for anthracene in water–ethanol solutions in the presence of luciferase (25). In their analysis, only one correlation time was resolved.

For fluorophores in a rotationally diffusion-constrained medium, the anisotropy correlation time is expected to approach infinity. However, our result shows that anthracene bound in MIPs and non-MIPs has a fast anisotropy decay (Table 2), which is probably due to efficient energy transfer between the anthracene and the polyurethane. In support of this idea, the anisotropy of a different fluorophore imprinted in a different polymer system was investigated as a comparison. 1.75 mg 9-dansyladenine was dissolved in a mixture of 50 mg polystyrene (PS) and 8.4 mg 4-azido-2,3,5,6-tetrafluorobenzoic acid (PFPA-COOH) in 1 mL chloroform. The polymer mixture solutions were spin-coated on silicon wafers followed by UV irradiation to form a thin polymer film (28). Polymer films with and without dansyladenine were compared. Dansyladenine–polymer film had emission fluorescence of 450–570 nm at an excitation of 360 nm, while the fluorescence of PS + PFPA-COOH film in the absence of 9-dansyladenine was ~50 times weaker. Our results showed that the time-resolved anisotropy of dansyladenine-polymer did not decay within 50 ns and had a limiting anisotropy of 0.2. Since polystyrene has nearly zero absorption in the fluorescence range of dansyladenine, the anisotropy decay was not observed in this polymer system.

Rebound-MIPs and rebound-non-MIPs had the same fluorescence lifetime of 0.64 ns and similar fast correlation times (1.2 and 1.5 ns). However, rebound-MIPs have much shorter slow correlation time (11.5 ns) than the rebound-non-MIPs (110 ns). We are not sure which are the most important factors affecting the fluorescence lifetime of the polymer systems, but we suspect that the distances between anthracene and polyurethane molecule are similar in the MIP or non-MIP systems for most (≥85%) of the molecules (Table 2). However, for a small proportion of the anthracene rebound in MIPs, the distances between the anthracene and the MIP backbone were shorter than that between the anthracene and non-MIPs.

One other possible explanation is that the fast correlation times arise from non-specific binding. However, according to our previous rebinding study (15), the specific binding to non-specific binding ratio was about 7:1 and rebound-MIPs exhibited higher fluorescence signals than rebound-non-MIPs. Therefore, the percentage of non-specific bindings in rebound-MIPs should be small. Wandelt *et al.* found a longer fluorescence lifetime for non-specific bindings, implying greater non-specific binding distances between the dipoles in their MIP system (14). Nonetheless, different MIPs systems may have totally different binding structures. Different porosity and polarity of the MIP environment may induce different non-specific binding environments. In our MIP system, the only forces present are van der Waals' force and π–π stabilization forces that exist between the aromatic structures. Since both polyurethane and anthracene have aromatic structures and MIPs and non-MIPs have similar percentages of porogen (DMF) that may create similar solvent cage environments, it is highly likely that our non-MIPs had similar binding environments to MIPs for anthracene. Further investigation is needed to support this hypothesis.

The anisotropy of the polymer solutions increases during polymerization and fits a simple exponential polymerization model (Fig. 6). Since the viscosity increases during polymerization, this anisotropy probably reflects the viscosity of the fluorophore local environment (29). When the polymer solutions were initially mixed, the fluorophores were still in a free-rotation environment; the initial anisotropy was close to 0. As the mixture polymerized, the cross-linking and imprinting process inhibited the fluorophores from rotating freely. As the polymerization continued, the proportion of rigidly-bound fluorophores increased, and therefore the anisotropy increased. Assume that $fI_{\parallel}$ and $fI_{\perp}$ is the parallel and perpendicular fluorescence from bound fluorophores, and $(1-f)I_{\parallel}$ and $(1-f)I_{\perp}$ is the proportion arising from unbound fluorophores. Since the unbound fluorophores are rotationally free, the emission will be independent of the plane of incidence, therefore:

$$(1-f)I_{\parallel} = (1-f)I_{\perp}$$

The anisotropy of partially polymerized samples becomes:

$$r = \frac{fI_{\parallel} + (1-f)I_{\parallel} - fI_{\perp} - (1-f)I_{\perp}}{I_{\parallel} + 2I_{\perp}} = \frac{f(I_{\parallel} - I_{\perp})}{I_{\parallel} + 2I_{\perp}}$$

Thus as the fraction of bound fluorophores f increases, so will the degree of anisotropy r.

CONCLUSIONS

We have investigated both steady-state and time-resolved fluorescence anisotropies of anthracene-imprinted polyurethane. For this MIP system, we found that MIPs and non-MIPs have the same steady-state anisotropy. We observed that analytes rebound in the polymer system had a shorter fluorescence lifetime and a shorter fast rotational correlation time than that

initially imprinted in polymers, suggesting a short-distance and tight binding between the analyte and the polymer when they rebound. However, further investigation is necessary to confirm this hypothesis. Finally, we observed that the steady-state anisotropy of polymer solutions increased with the extent of polymerization. The steady-state anisotropy may provide an alternative method to observe the polymerization process or to measure the viscosity changes of fluorophore solutions with the advantages of *in situ* measurement.

Acknowledgements

The fluorescence measurements were performed at the W. R. Wiley Environmental Molecular Sciences Laboratory, a national scientific user facility sponsored by the US Department of Energy's Office of Biological and Environmental Research and located at Pacific Northwest National Laboratory. PNNL is operated for the Department of Energy by Battelle. The authors would like to thank the help of Dr Alan Joly at PNNL for the use of the time-resolved instrument. We thank Dr Steve Jacques at the Department of Biomedical Engineering, OHSU, for his helpful suggestions and use of his filters. We thank Dr Robert W. Redmond at the Wellman Center for Photomedicine, Massachusetts General Hospital and Harvard Medical School, for his helpful suggestions. This work was supported by the NIH Grant NIH-CI-R24-CA84587-03.

REFERENCES

1. Vlatakis G, Andersson LI, Muller R, Mosbach K, Drug assay using antibody mimics made by molecular imprinting. *Nature* 1993; **361**: 645–647.
2. Kriz D, Ramstrom O, Mosbach K. Molecular imprinting—new possibilities for sensor technology. *Anal. Chem.* 1997; **69**: A345–A349.
3. Watabe Y, Hosoya K, Tanaka N *et al.* Novel surface-modified molecularly imprinted polymer focused on the removal of interference in environmental water samples. *Chem. Lett.* 2004; **33**: 806–807.
4. Huang YC, Lin CC, Liu CY, Preparation and evaluation of molecularly imprinted polymers based on 9-ethyladenine for the recognition of nucleotide bases in capillary electrochromatography. *J. Chromatogr. A* 2004; **25**: 554–561.
5. Ye L, Haupt K. Molecularly imprinted polymers as antibody and receptor mimics for assays, sensors and drug discovery. *Anal. Bioanal. Chem.* 2004; **378**: 1887–1897.
6. Gutierrez-Fernandez S, Lobo-Castanon MJ, Miranda-Ordieres AJ *et al.* Molecularly imprinted polyphosphazene films as recognition element in a voltammetric rifamycin SV sensor. *Electroanalysis* 2001; **13**: 399–1404.
7. Huang HC, Lin CI, Joseph AK, Lee YD, Photo-lithographically impregnated and molecularly imprinted polymer thin film for biosensor applications. *Electrophoresis* 2004; **1027**: 263–268.
8. Marx S, Zaltsman A, Turyan I, Mandler D. Parathion sensor based on molecularly imprinted sol–gel films. *Anal. Chem.* 2004; **76**: 120–126.
9. Haupt K, Mosbach K. Molecularly imprinted polymers and their use in biomimetic sensors. *Chem. Rev.* 2000; **100**: 2495–2504.
10. Guo HS, He X. Study on the binding characteristics of molecular imprinted polymer selective for cefalexin in aqueous media. *Chin. J. Anal. Chem.* 2000; **28**: 1214–1219.
11. Quaglia M, Lorenzi ED, Sulitzky C, Massolini G, Sellergren B. Surface initiated molecularly imprinted polymer films: a new approach in chiral capillary electrochromatography. *Analyst* 2001; **126**(9): 1495–1498.
12. Yilmaz E, Mosbach K, Haupt K. Influence of functional and cross-linking monomers and the amount of template on the performance of molecularly imprinted polymers in binding assays. *Anal. Commun.* 1999; **36**: 167–170.
13. Dickert FL, Tortschanoff M. Molecularly imprinted sensor layers for the detection of polycyclic aromatic hydrocarbons in water. *Anal. Chem.* 1999; **71**: 4559–4563.
14. Wandelt B, Turkewitsch P, Wysocki S, Darling GD. Fluorescent molecularly imprinted polymer studied by time-resolved fluorescence spectroscopy. *Polymer* 2002; **43**: 2777–2785.
15. Chen YC, Brazier JJ, Yan M, Bargo PR, Prahl SA. Fluorescence-based optical sensor design for molecularly imprinted polymers. *Sens. Actuators B Chem.* 2004; **102**: 107–116.
16. Lakowicz JR. *Principles of Fluorescence Spectroscopy*. Kluwer Academic/Plenum: New York, 1999.
17. Anderson J, Nelson J, Reynolds C *et al.* Steady-state and frequency-domain lifetime measurements of an activated molecular imprinted polymer imprinted to dipicolinic acid. *J. Fluoresc.* 2004; **14**: 269–274.
18. Przhonska O, Bondar M, Gallay J *et al.* Photophysics of dimethylamino-substituted polymethine dye in polymeric media. *J. Photochem. Photobiol. B Biol.* 1999; **52**: 19–29.
19. Morrison ME, Dorfman RC, Clendening WD *et al.* Quenching kinetics of anthracene covalently bound to a polyelectrolyte. 1. Effects of ionic strength. *J. Phys. Chem.* 1994; **98**: 5534–5540.
20. Pokorná V, Výprachtický D, Pecka J, Mikeš F. Time-resolved emission anisotropy of anthracene fluorophore in the backbone of stereoregular poly(methyl methacrylate). *Macromol. Chem. Phys.* 2001; **202**: 155–162.
21. Tleugabulova D, Duft AM, Brook MA, Brennan JD. Monitoring solute interactions with poly(ethylene oxide)-modified colloidal silica nanoparticles via fluorescence anisotropy decay. *Langmuir* 2004; **20**: 101–108.
22. Stenger DA, Georger JH, Dulcey CS *et al.* Coplanar molecular assemblies of aminoalkylsilane and perfluorinated alkylsilane—characterization and geometric definition of mammalian cell adhesion and growth. *J. Am. Chem. Soc.* 1992; **114**: 8435–8442.
23. Lloyd CH, Scrimgeour SN, Chudek JA, Hunter G, MacKay RL, The application of magnetic resonance microimaging to the visible light curing of dental resins. Part 2. Dynamic imaging by the FLASH-MOVIE pulse sequence. *Dent. Mater.* 2001; **17**: 170–177.
24. Cohen ME, Leonard DL, Charlton DG, Roberts HW, Ragain JC Jr. Statistical estimation of resin composite polymerization sufficiency using microhardness. *Dent. Mater*. 2004; **20**: 158–166.
25. Kudryasheva NS, Nemtseva EV, Visser A, van Hoek A. Interaction of aromatic compounds with *Photobacterium leiognathi* luciferase: fluorescence anisotropy study. *Luminescence* 2003; **18**: 156–161.
26. Sturgeon RJ, Schulman SG. Steric inhibition of conjugation in lowest excited singlet state of 9-anthramide by hydrogen bond donor solvents: role of solvent in chemical structure. *J. Pharm. Sci.* 1976; **65**: 1833–1835.
27. Lampert RA, Chewter LA, Phillips D *et al.* Standards for nanosecond fluorescence decay time measurements. *Anal. Chem.* 1983; **55**: 68–73.
28. Yan M, Harnish B. A simple method for the attachment of polymer films on solid substrates. *Adv. Mater.* 2003; **15**: 244–248.
29. Smith TA, Bajada LM, Dunstan DE. Fluorescence polarization measurements of the local viscosity of hydroxypropyl guar in solution. *Macromolecules* 2002; **35**: 2736–2742.

